Detection of spin coupling in iron nanoparticles with small angle neutron scattering

Y. Ijiri[a] and C. V. Kelly
Oberlin College, Department of Physics and Astronomy, Oberlin, Ohio 44074

J. A. Borchers
NIST Center for Neutron Research, National Institute of Standards and Technology, Gaithersburg, Maryland 20899

J. J. Rhyne
Lujan Neutron Scattering Center, Los Alamos National Laboratory, Los Alamos, New Mexico 87545

D. F. Farrell and S. A. Majetich[b]
Department of Physics, Carnegie Mellon University, Pittsburgh, Pennsylvania 15213

(Received 14 February 2005; accepted 9 May 2005; published online 7 June 2005)

Aggregates of monodisperse iron-based nanoparticles were investigated by small-angle neutron scattering. The field dependence of the scattering intensity showed marked differences for particles depending on size and degree of oxidation. The angular dependence of the intensity indicated magnetic regions within an oxidized sample with spins perpendicular to the applied field, which dominated the scattering at the diffraction peak. The unexpected results are interpreted in terms of an iron core that is exchange coupled to an iron oxide shell. © *2005 American Institute of Physics*. [DOI: 10.1063/1.1947906]

Monodisperse magnetic nanoparticles form an intriguing system for the study of size-dependent properties, interparticle magnetic interactions, and potential data storage media.[1–5] In dilute ferrofluids similar nanoparticles are magnetostatically coupled into a spin glasslike state[2] but the nature and extent of interactions at higher densities are not well understood. Small-angle neutron scattering (SANS) is one of the few tools well suited to characterize this magnetic coupling as well as its length scales.[6–8] By applying SANS to ordered samples with more uniform particle size and separation, we should obtain a more precise understanding of the relevant intra- and interparticle correlations. Here, we examine these issues for dense assemblies of Fe nanoparticles, similar to those investigated previously in dilute suspensions.[9] Our results reveal that for dense compacts, SANS is highly sensitive to the degree of oxidation. In particular, for greater oxidation, we observe an unexpected high-field distortion to the scattering, consistent with perpendicularly coupled iron-iron oxide spins.

Iron nanoparticles were prepared using solution chemistry methods that have been described previously.[5] Three samples were made with iron-containing core diameters of 5.7 ± 0.2 nm, 8.2 ± 0.4 nm, and 8.6 ± 0.7 nm, as determined by transmission electron microscopy. The typical nearest-neighbor spacing between the edges of particle cores was ~2.5 nm. The 5.7 and 8.6 nm particles had minimal oxidation, which is indicated by high values for the saturation magnetization (nearly 80–90% of bulk) and no measurable shift in the 10 K field-cooled hysteresis loop. While similar in size to the 8.6 nm particles, the 8.2 nm particles were partially oxidized as a result of slightly greater exposure to oxygen during handling beyond the typical <1 ppm level. For such particles, the specific magnetization is reduced slightly (~60% of bulk) and evidenced at low temperature by a ~200 Oe shift in the field-cooled hysteresis loop.[10] For the SANS experiments, a hexane dispersion of the nanoparticles was evaporated in an aluminum sample holder, which was then sealed with indium prior to removal from an argon glove box. The resulting nanoparticle films were a few millimeters thick. Under these conditions, the particles have local ordering, but are unlikely to be in long-range periodic arrays.

SANS experiments were conducted at the NG-3 and NG-7 beam lines at the NIST Center for Neutron Research using neutrons with a wavelength λ of either 0.5 or 0.8 nm. Data were collected in transmission with a two-dimensional detector at two different distances, in order to span the range of scattering vectors, $Q=4\pi\sin\theta/\lambda$, from ~0.05 to 2 nm^{-1}. Measurements were taken between 5 and 295 K and in magnetic fields ranging from 0 to 5.0 T. The field was applied in the plane of the film and normal to the neutron beam.

As illustrated in Fig. 1, the SANS signal for the samples showed a diffraction peak in the high Q range. The peaks corresponded to spacings of $L=2\pi/Q$ of 6.5 ± 1.5 nm and of 10 ± 2 nm for the 5.7 nm and 8.2 nm particles, respectively. These spacings are consistent with the distances between (111) planes of a face-centered-cubic lattice of nanoparticles, which for these samples are ~6.7 nm and ~8.7 nm. The magnitude of the peak exhibited some temperature dependence, as expected for magnetic particle scattering.

The second notable feature of the scattering in Fig. 1 is the significant increase in intensity at low Q values as the temperature decreases. The Q dependence here was neither Lorentzian (as expected for dynamical spin fluctuations) nor Lorentzian squared (as expected for uncorrelated particle moments and observed previously in Fe nanoparticles in an alumina matrix).[6] The onsets for field-dependent deviations with Q have previously been interpreted in terms of upper limits for the magnetic correlation length scales in nanocrys-

[a]Electronic mail: yumi.ijiri@oberlin.edu
[b]Electronic mail: sm70@andrew.cmu.edu

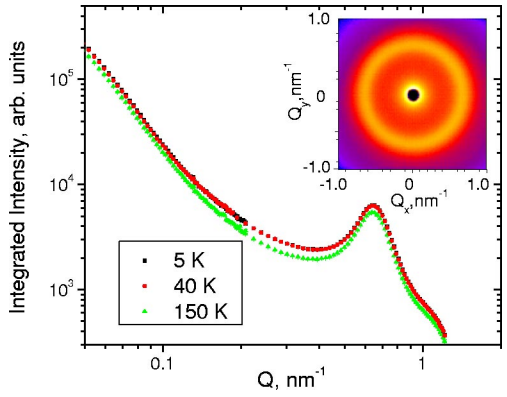

FIG. 1. (Color online) Radially averaged SANS intensity vs scattering vector for 8.2 nm core particles at different temperatures in zero applied field. Data above 150 K become distorted due to melting of residual hexane. Inset depicts two-dimensional plot of intensity, showing a diffraction ring at $Q \sim 0.63$ nm^{-1} and an increase in the intensity at low Q. Data for 5.7 nm particles show similar features with a ring at $Q \sim 1.0$ nm^{-1}.

talline metals.[11] With a similar approach, we can calculate a maximum magnetic length scale of ~20 nm ($Q \sim 0.4$ nm^{-1}) for the 5.7 nm particles and ~70 nm ($Q \sim 0.09$ nm^{-1}) for the 8.2 nm particles in zero-applied field.

Applied magnetic fields led to significant changes in the SANS intensity at the diffraction peaks, the magnitudes of which depended on the particle size. To show this most clearly, we plot in Fig. 2 the angular dependence at 5 K of the intensity difference at the diffraction peak position, $\Delta I = I(5\mathrm{T}) - I(0)$, scaled against the radially averaged intensity I_{ave}. Only the components of the magnetization perpendicular to the scattering vector contribute to the magnetic neutron scattering. For a ferromagnet aligned in an applied field H, that scattering should be $\alpha \sin^2\alpha$, where α is the angle between Q and H. The 5.7 nm particles show a very small decrease in scattering for Q directions parallel to the field and a small increase perpendicular to the field [Fig. 2(a)]. The $\sin^2\alpha$ behavior was evident only below the blocking

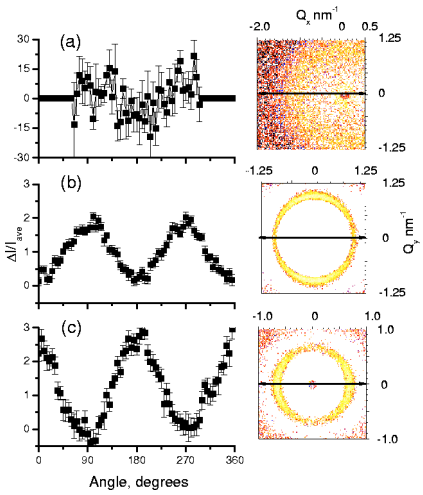

FIG. 2. (Color online) Angular dependence of the difference between the 5 T and 0 T SANS intensity at 5 K for (a) minimally oxidized 5.7 nm, (b) minimally oxidized 8.6 nm, and (c) partially oxidized 8.2 nm nanoparticles, taken at the respective diffraction peaks. The data are scaled against the radially averaged intensity. The angle corresponds to the angular direction of Q, relative to the magnetic field, which was applied in the horizontal direction, corresponding to angles of 0° (360°) or 180°, as shown in the accompanying two-dimensional subtracted intensity plots.

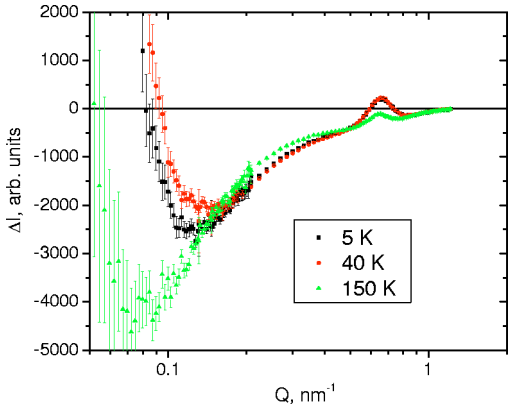

FIG. 3. (Color online) Radially averaged SANS intensity for (5 T–0 T) as a function of scattering vector at different temperatures for the 8.2 nm partially oxidized nanoparticles.

temperature of ~30 K and in high magnetic fields. Minimally oxidized 8.6 nm particles show a much stronger $\sin^2\alpha$ behavior, as expected for ferromagnetic Fe cores that align parallel to the applied field [Fig. 2(b)]. Although evident in more moderate applied fields (~0.1 T), the effect was most prominent at high fields with temperatures below the blocking temperature for these particles (~80 K).

When the nanoparticles have some further oxidation, however, the SANS behavior is markedly changed. Partially oxidized 8.2 nm particles showed a noticeable *increase* in scattering along the field direction at the diffraction peak [Fig. 2(c)]. The effect was most pronounced again at high field and below the blocking temperature. At low Q, a similar $\cos^2\alpha$ dependence was observed, whereas in the medium Q region (0.1–0.5 nm^{-1}), this angular behavior was absent, and the scattering was isotropic. Figure 3 illustrates the field-induced changes in the SANS signal in more detail, plotting the intensity differences as a function of Q, in analogy to recent resonant x-ray scattering work on Co nanoparticles.[12] Here, at both low and high Q, the scattering intensity increased with field, while in the medium Q range, the scattering intensity decreased as expected for a ferromagnet, aligning in the applied field. The majority of the field-dependent changes occur between 40 K and 150 K, which is consistent with the magnetization drop above the blocking temperature (~80 K).

Deviations from $\sin^2\alpha$ dependencies have been observed in several other systems.[13–16] In CrFe (Ref. 13) and certain rare-earth alloys,[14] it was interpreted in terms of different sized groups of interacting spins. The smaller superparamagnetic clusters aligned in moderate fields, but larger ones with perpendicular magnetic moments remained unaligned. However, such a spin glass model should result in intensity changes with field for *all* Q, unlike what was observed in our data. We note also that a $\cos^2\alpha$ dependence has been previously observed in *low* magnetic fields (~1–100 mT), stemming from either a competing magnetic anisotropy as seen in melt-spun Vitroperm[15] or a competing exchange anisotropy as seen in nanocrystalline Fe with a trace amount of iron oxide.[16] In both cases, at higher magnetic fields, the expected $\sin^2\alpha$ dependence was found.

In our nanoparticles, we expect that ferrimagnetic Fe_3O_4, γ-Fe_2O_3, or other Fe–O compounds have formed at the surface. Just as with a ferromagnet coupled to an antiferromagnet,[17] we have observed evidence of exchange

coupling between the ferromagnetic Fe core and a ferrimagnetic iron oxide shell, with a shift in the field-cooled hysteresis loop of ~200 Oe for partially oxidized 8 nm particles.[10] Recent work has shown that the interfacial antiferromagnetic spins near the interface with a ferromagnet are sometimes perpendicular to the ferromagnetic moments.[18] In addition, canted surface spins have been observed previously in ferrite nanoparticles with applied fields of order 10 T.[19]

We thus interpret our unusual SANS data in Figs. 2 and 3 in terms of different responses from nanoparticle cores and surrounding oxide shells. Specifically, the spins in the magnetically soft iron cores are expected to align at low fields while those in the oxide shells remain in a spin-flop state even at 5 T. The effect of such an arrangement on the scattering is particularly prominent at the interparticle peak, which stems from the local ordering in the nanoparticles and allows for a more quantitative analysis than possible in previous work.[16] We can focus on the magnetic effect by subtracting the structural contribution estimated from the higher-temperature data and computing the ratio (R) of peak intensities parallel versus perpendicular to the applied field, sector averaging over ±5°. For the partially oxidized 8.2 nm particles at the highest field (5 T) and lowest temperature (5 K), R is 1.5 ± 0.1 versus 0.57 ± 0.07 for the less oxidized 8.6 nm particles.

To estimate the corresponding degrees of oxidation, let us assume that the magnetic intensity parallel to the field stems only from the coherent interference of the iron oxide spins due to the array spacing, and that the magnetic intensity perpendicular to the field stems from that same periodicity in the iron cores. The ratio R then should be proportional to the $\mu^2_{\text{Fe-O}}/\mu^2_{\text{Fe}}$, where μ is the magnetic moment. Using bulk values of iron and magnetite magnetization and density, we estimate the oxide shell thicknesses of ~1.8 nm versus ~1.55 nm for the more and less oxidized particles, respectively. Clearly, these values would be affected by factors, such as deviations in the magnetization from bulklike behavior and varying degrees of spin canting in either the shell or core. Nevertheless, the core-shell model applied to the diffraction peak gives reasonable values for the size of the spin-flopped regions and highlights the ability of SANS to detect small changes in spin alignment.

The core-shell arrangement can also be used to interpret the field-dependent changes at other Q values. Corresponding to length scales on the order of the particle diameter, the medium Q region is more similar to a standard ferromagnet, with intensity decreasing on application of an applied field, as shown in Fig. 3. The low Q region reflects lengths extending over multiple particles. If the moments of neighboring particle cores are aligned, and within a particle the shell spins are perpendicular to the core, then there will also be long-range correlations of the oxide spins versus the core spins, reflected in a signal similar to, albeit, weaker than the diffraction peak.

In summary, we have used SANS to uncover oxidation-dependent differences in spin arrangements for iron-based nanoparticles and, similar to recent results on magnetic media,[20] we have analyzed our data in terms of a core-shell geometry. The results highlight the sensitivity of SANS to relatively subtle changes in oxidation and the importance of such effects in understanding and manipulating magnetic nanoparticles.

This work was supported for some of the authors by the National Science Foundation No. CTS-0227645 (S. A. M.), the American Chemical Society Petroleum Research Fund 40049-B5M (Y. I.) and 37578-AC5 (S.A.M), Research Corporation CC5820 (Y. I.), and the University of Missouri Research Board (J. J. R.). This work utilized facilities supported in part by the National Science Foundation under Agreement No. DMR-9986442.

[1] J. L. Dormann, D. Fiorani, and E. Tronc, Adv. Chem. Phys. **98**, 283 (1997) and references therein.
[2] T. Jonsson, P. Svedlindh, and M. F. Hansen, Phys. Rev. Lett. **81**, 3976 (1998).
[3] V. Russier, H. Doyle, C. Petit, J. Legrand, and M. P. Pileni, Phys. Rev. B **62**, 3910 (2000).
[4] G. A. Held, G. Grinstein, H. Doyle, S. Sun, and C. B. Murray, Phys. Rev. B **64**, 012408 (2001).
[5] D. Farrell, S. A. Majetich, and J. P. Wilcoxon, J. Phys. Chem. **107**, 11022 (2003); D. Farrell, Y. Ding, and S. A. Majetich, J. Appl. Phys. **95**, 6636 (2004).
[6] C. Bellouard, I. Mirebeau, and M. Hennion, Phys. Rev. B **53**, 5570 (1996).
[7] J. Weissmüller, A. Michels, J. G. Barker, A. Wiedenmann, U. Erb, and R. D. Shull, Phys. Rev. B **63**, 214414 (2001).
[8] M. F. Toney, K. A. Rubin, S. Choi, and C. J. Glinka, Appl. Phys. Lett. **82**, 3050 (2003).
[9] K. Butter, A. Hoell, A. Wiedenmann, A. V. Petukhov, and G.-J. Vroege, J. Appl. Crystallogr. **37**, 847 (2004).
[10] D. F. Farrell, Ph.D. dissertation, Carnegie Mellon University, 2003.
[11] J. F. Löffler, H. B. Braun, W. Wagner, G. Kostorz, and A. Wiedenmann, Mater. Sci. Eng., A **304**, 1050 (2001).
[12] J. B. Kortright, O. Hellwig, K. Chesnel, S. Sun, and E. E. Fullerton, Phys. Rev. B **71**, 012402 (2005).
[13] S. K. Burke, R. Cywinski, and B. D. Ramford, J. Appl. Crystallogr. **11**, 644 (1978).
[14] J. J. Rhyne, IEEE Trans. Magn. **21**, 1990 (1985).
[15] A. Michels, R. N. Viswananth, and J. Weissmüller, Europhys. Lett. **64**, 43 (2003).
[16] J. F. Löffler, W. Wagner, H. van Swygenhoven, and A. Wiedenmann, Nanostruct. Mater. **9**, 331 (1997).
[17] W. H. Meiklejohn and C. P. Bean, Phys. Rev. **105**, 904 (1957).
[18] Y. Ijiri, J. Phys.: Condens. Matter **14**, 947 (2002) and references therein.
[19] R. H. Kodama, A. E. Berkowitz, E. J. McNiff, and S. Foner, Phys. Rev. Lett. **77**, 394 (1996).
[20] S. L. Lee, T. Thomson, F. Y. Ogrin, C. Oates, M. Wismayer, C. Dewhurst, R. Cubitt, and S. Harkness, Mater. Res. Soc. Symp. Proc. **803**, GG4.4.1 (2004).